PAPER P-789

THE QUENCHING OF $O(^1D)$ BY N_2 AND RELATED REACTIONS

Edward R. Fisher
Wayne State University

Ernest Bauer

December 1971

INSTITUTE FOR DEFENSE ANALYSES
SCIENCE AND TECHNOLOGY DIVISION

UNCLASSIFIED

Security Classification

DOCUMENT CONTROL DATA - R & D

(Security classification of title, body of abstract and indexing annotation must be entered when the overall report is classified)

1 ORIGINATING ACTIVITY (Corporate author)

INSTITUTE FOR DEFENSE ANALYSES
400 Army Navy Drive
Arlington, Virginia 22202

2a. REPORT SECURITY CLASSIFICATION

UNCLASSIFIED

2b GROUP

--

3 REPORT TITLE

The Quenching of $O(^1D)$ by N_2 and Related Reactions

4 DESCRIPTIVE NOTES (Type of report and inclusive dates)

Paper P-789 - December 1971

5 AUTHOR(S) (First name, middle initial, last name)

Edward R. Fisher, Ernest Bauer

6 REPORT DATE

December 1971

7a. TOTAL NO OF PAGES

42

7b. NO OF REFS

31

8a. CONTRACT OR GRANT NO

DAHC15 67 C 0011

b. PROJECT NO

ARPA Assignment 5

c

d.

9a. ORIGINATOR'S REPORT NUMBER(S)

P-789

9b. OTHER REPORT NO(S) (Any other numbers that may be assigned this report)

None

10 DISTRIBUTION STATEMENT

Approved for public release; distribution unlimited

11 SUPPLEMENTARY NOTES

None

12. SPONSORING MILITARY ACTIVITY

Advanced Research Projects Agency
Arlington, Virginia 22209

13 ABSTRACT

As an extension of earlier work on the quenching of electronically excited alkali metal atoms by N_2 and CO, which uses a model of curve crossing involving an ionic intermediate state, here we treat the quenching of $O(^1D)$ by N_2, a process which proceeds by curve crossing of covalent states. The model is also applied to the vibrational relaxation of N_2 in collision with $O(^3P)$ atoms and to the unimolecular decomposition of N_2O. The order of magnitude of the rate constants for all 3 processes can be explained by the present model, using the same value of the electronic coupling potential for the curve-crossing process; this value is significantly larger than the corresponding value for isolated $O(^3P)$ and $O(^1D)$ atoms. In the quenching of $O(^1D)$ by N_2, the electronic-vibrational coupling is weak, channeling less that 5% of the electronic quantum into vibrational levels of N_2, but the quenchant N_2 is likely to be rotationally excited. The vibrational relaxation of N_2 by oxygen atoms arising due to curve crossing rather than to adiabatic ("Landau-Teller") collisions has a significant activation energy, ~0.8 ev, so that the rate coefficient for vibrational relaxation due to curve crossing is expected to show a strong temperature dependence and to dominate at temperatures above 6000K.

DD FORM 1 NOV 68 1473

UNCLASSIFIED

Security Classification

The work reported in this document was conducted under contract DAHC15 67 C 0011 for the Department of Defense. The publication of this Paper does not indicate endorsement by the Department of Defense, nor should the contents be construed as reflecting the official position of that agency.

14 KEY WORDS	LINK A		LINK B		LINK C	
	ROLE	WT	ROLE	WT	ROLE	WT
curve crossing						
quenching of $O(^1D)$ by N_2						
unimolecular decomposition of N_2O						
vibrational relaxation of N_2						

PAPER P-789

THE QUENCHING OF $O(^1D)$ BY N_2 AND RELATED REACTIONS

Edward R. Fisher
Wayne State University

Ernest Bauer

December 1971

INSTITUTE FOR DEFENSE ANALYSES
SCIENCE AND TECHNOLOGY DIVISION
400 Army-Navy Drive, Arlington, Virginia 22202

Contract DAHC15 67 C 0011
ARPA Assignment 5

ACKNOWLEDGEMENTS

We should like to thank Dr. Morris Krauss for providing the information regarding electronic states of the N_2O molecule and effective transition matrix elements, and Drs. F. T. Smith, F. R. Gilmore, R. E. Olson, and J. R. Peterson for most helpful discussions.

FOREWORD

The state of the earth's upper atmosphere under normal and disturbed conditions is of considerable importance for a variety of military applications, ranging from ionospheric radio wave propagation to high-altitude nuclear explosions. The biggest reservoir of energy storage in the atmospheric E-region is provided by the Schumann-Runge photodissociation of molecular oxygen, which yields one oxygen atom in the excited ^1D state. This excited atom is rapidly de-excited ("quenched") by collision with atmospheric molecular nitrogen. The question of the possible vibrational excitation of nitrogen by this process and of its de-excitation by the vibration-translation energy transfer between N_2 and O (which is also studied here) is a very important one, since the atmospheric E-region is far from thermodynamic equilibrium, and the effective vibrational population, which is partly determined by these two processes, may affect both the neutral and ionic atmospheric chemistry (in particular the de-ionization) as well as the airglow.

The present calculation of these reactions provides the basis for an experimental investigation of these same processes which is now being conducted at Stanford Research Institute under ARPA contract; the present calculation guides and complements those measurements as well as providing a basis for further experimental and theoretical work in this area.

This work was performed under sponsorship of the Strategic Technology Office of the Advanced Research Projects Agency.

ABSTRACT

As an extension of earlier work on the quenching of electronically excited alkali metal atoms by N_2 and CO, which uses a model of curve crossing involving an ionic intermediate state, here we treat the quenching of $O(^1D)$ by N_2, a process which proceeds by curve crossing of covalent states. The model is also applied to the vibrational relaxation of N_2 in collision with $O(^3P)$ atoms and to the unimolecular decomposition of N_2O. The order of magnitude of the rate constants for all three processes can be explained by the present model, using the same value of the electronic coupling potential for the curve-crossing process; this value is significantly larger than the corresponding value for isolated $O(^3P)$ and $O(^1D)$ atoms. In the quenching of $O(^1D)$ by N_2, the electronic-vibrational coupling is weak, channeling less than 5 percent of the electronic quantum into vibrational levels of N_2, but the quenchant N_2 is likely to be rotationally excited. The vibrational relaxation of N_2 by oxygen atoms arising due to curve crossing rather than to adiabatic ("Landau-Teller") collisions has a significant activation energy, ~ 0.8 ev, so that the rate coefficient for vibrational relaxation due to curve crossing is expected to show a strong temperature dependence and to dominate at temperatures above $600^{\circ}K$.

CONTENTS

I. INTRODUCTION

In collisions of atoms and molecules at elevated temperatures, the flow of energy between electronic and vibrational, rotational, and translational states, i.e., quenching processes, can have significant effects on both transient and steady-state molecular properties. Recently, calculations were presented on the quenching of electronically excited alkali atoms by simple diatomics (Refs. 1 and 2), e.g.,

$$Na(3^2P) + N_2 \rightarrow \{Na^+ - N_2^-\} \rightarrow Na(3^2S) + N_2(v) + K.E. \qquad (1)$$

where it was shown that the vibration-electronic coupling was strong due to the unstable intermediate state, which is largely ionic in character. As an outgrowth of this work, it was recognized that a similar curve-crossing mechanism would be operative in the relaxation of vibrational energy in N_2 during collisions with alkali atoms;

$$N_2(v) + Na(3^2S) \rightarrow \{N_2^- - Na^+\} \rightarrow N_2(v' < v) + Na(3^2S) + K.E. \qquad (2)$$

These calculations (Ref. 3) demonstrated that this vibrational relaxation process may have significantly larger cross sections than other vibration-translation energy transfer processes which do not involve a curve crossing.

Reactions (1) and (2) proceed by the crossing of potential energy curves (a Landau-Zener process) through an ionic intermediate state (Ref. 4), although the quenching model developed in the earlier studies is not restricted to the crossing of ionic and covalent states. In this paper, a quenching reaction is investigated which proceeds

entirely through the crossing of covalent potential energy curves. By analogy to the ionic quenching studies, the following reactions all proceed through the same or similar potential energy curve crossings (Ref. 5);

$$N_2O(X^1\Sigma^+) \rightarrow N_2(X^1\Sigma_g^+) + O(^3P) \quad \text{(unimolecular decomposition)} \quad (3)$$

$$O(^1D) + N_2 \rightarrow \{N_2O\} \rightarrow O(^3P) + N_2(v, J) + \text{K.E.} \quad \text{(quenching of } O(^1D) \text{ by } N_2) \quad (4)$$

$$O(^3P) + N_2(v) \rightarrow \{N_2O\} \rightarrow O(^3P) + N_2(v' < v) + \text{K.E.}$$

(N_2 vibrational relaxation by O atoms). (5)

Thus, in the present work a simple but unified analysis of reactions (3) - (5) is presented, based on the same electronic states of N_2O. In Section II an analysis is given of the potential energy curves of low-lying electronic states of the N_2O system, and then in Section III the nature of the quantum mechanical collision problem, in particular the curve crossings and the magnitude of the transition matrix element, is discussed. The specific processes (3), (4), and (5) are discussed in Sections IV, V, and VI, respectively, and a concluding discussion is given in Section VII.

The present covalent problem has considerable differences from the previous ionic problem, arising from the differences between short-range (valence) versus long-range (Coulomb) interactions. For an ionic intermediate, a long-range crossing (Ref. 6) occurs due to the Coulomb interaction, e^2/R; and the transition matrix element at the crossing is a function of the crossing distance (Refs. 7 and 8). Further, because of the long-range interaction, the distance $R(Na\text{-}N_2)$ or $R(Na^+ - N_2^-)$ is significantly greater than the distance R(N - N), and thus the geometrical orientation of the Na relative to N_2, or the angle N-$\hat{N}$-Na, is relatively unimportant. However, for

the covalent problem $R(N_2 - O) \cong R(N\text{-}N)$, and thus the orientation, as represented by the angle N-N-O, is of major importance for the potential energy surfaces. Further, the curve splitting or transition matrix element will presumably depend on effective quantum numbers and molecular symmetries rather than on the crossing distance. Also, because of these orientational factors, rotational excitation may be particularly important. These general characteristics of ionic versus covalent crossings are of importance if one wishes to extend the analysis to systems other than N_2O.

It is also appropriate to note the philosophy of the present work, which is to identify problem areas in a given class of important reactions by a semi-empirical approach, rather than to give a quantitative treatment. Such quantitative treatments will become possible within the next several years, with the development of powerful numerical techniques (Ref. 9), but at present there is still a significant gap between experimental data and understanding, which can be usefully filled by qualitative models such as that developed in this work.

In addition, it is important to note that reactions (4) and (5) are of considerable aeronomic importance. The quenching of $O(^1D)$ by atmospheric N_2 is a potentially important source of vibrational energy in the upper atmosphere (Refs. 10 and 11), while the relaxation of N_2 vibrational energy by O atoms may be an important loss mechanism. Measurements are available on both these reactions which show that the quenching rate coefficients are large (Refs. 12 and 13), of order 1/4 gas kinetic, while O atoms are known to be effective in relaxing N_2 vibrational energy (Ref. 14) at least in high-temperature systems.

The following conclusions can be drawn from the model developed in this paper: the vibration-electronic coupling in the quenching of $O(^1D)$ by N_2 is found to be weak, channeling only about 5 percent of the electronic quantum into vibrational levels of the quenchant

N_2, the quenchant N_2 is likely to be rotationally excited due to the importance of noncollinear configurations, and the relaxation of N_2 vibrational energy by $O(^3P)$ atoms is accompanied by a significant activation energy, ~ 0.8 ev, which indicates a strong temperature dependence in extrapolating measured high-temperature rate coefficients (Ref. 14) to lower temperatures.

II. POTENTIAL ENERGY CURVES

The ground state of the triatomic molecule N_2O is known to be a linear structure (N-N-O) of symmetry $^1\Sigma^+$, so that it clearly dissociates into $N_2(X^1\Sigma_g^+) + O(^1D)$ in order to conserve spin. On the other hand, $O(^1D)$ lies 1.98 ev above $O(^3P)$, so that at infinite separation the system $N_2(X^1\Sigma_g^+) + O(^3P)$ lies 1.98 ev below $N_2(X^1\Sigma_g^+) + O(^1D)$. There is thus no question that a curve crossing does occur. In fact the situation is rather complex: Peyerimhoff & Buenker (Ref. 16) have made quantum mechanical configuration interaction calculations for the system N-N-O as a function of the angle $\alpha = N\text{-}\hat{N}\text{-}O$, at the equilibrium internuclear separations $r_e(N\text{-}N) = 1.128$ A and $r_e(N\text{-}O) = 1.184$ A. It should be noted that the state assignments for electronically excited states of N_2O as listed in Herzberg (Ref. 15) do not agree with the calculations of Peyerimhoff and Buenker (Ref. 16); since the assignments in Herzberg are based on very limited data, it appears preferable to use the analysis of Peyerimhoff and Buenker.

For a collinear configuration, $\alpha = N\text{-}\hat{N}\text{-}O = 180^\circ$, as the $N_2(X^1\Sigma_g^+)$ and $O(^3P)$ systems are brought together, there are two electronic states $^3\Sigma^-$ and $^3\Pi$ of successively higher energy; when $N_2(X^1\Sigma_g^+)$ and $O(^1D)$ are brought together, there are three states $X^1\Sigma^+$, $^1\Delta$, $^1\Pi$. All these states are shown in Fig. 1 for $R(N\text{-}N) = r_e(N\text{-}N) = 1.128$ A. It should be noted that except for the $X^1\Sigma^+$ state, the curves for the other states have been faired in using the energy value from Ref. 16 for $R(N\text{-}O) = r_e(N\text{-}O) = 1.184$ A.

At small internuclear distances, the $^1\Pi$ and $^3\Pi$ states become Rydberg, i.e., highly repulsive, while the $^1\Delta$ and $^3\Sigma^-$ states are of

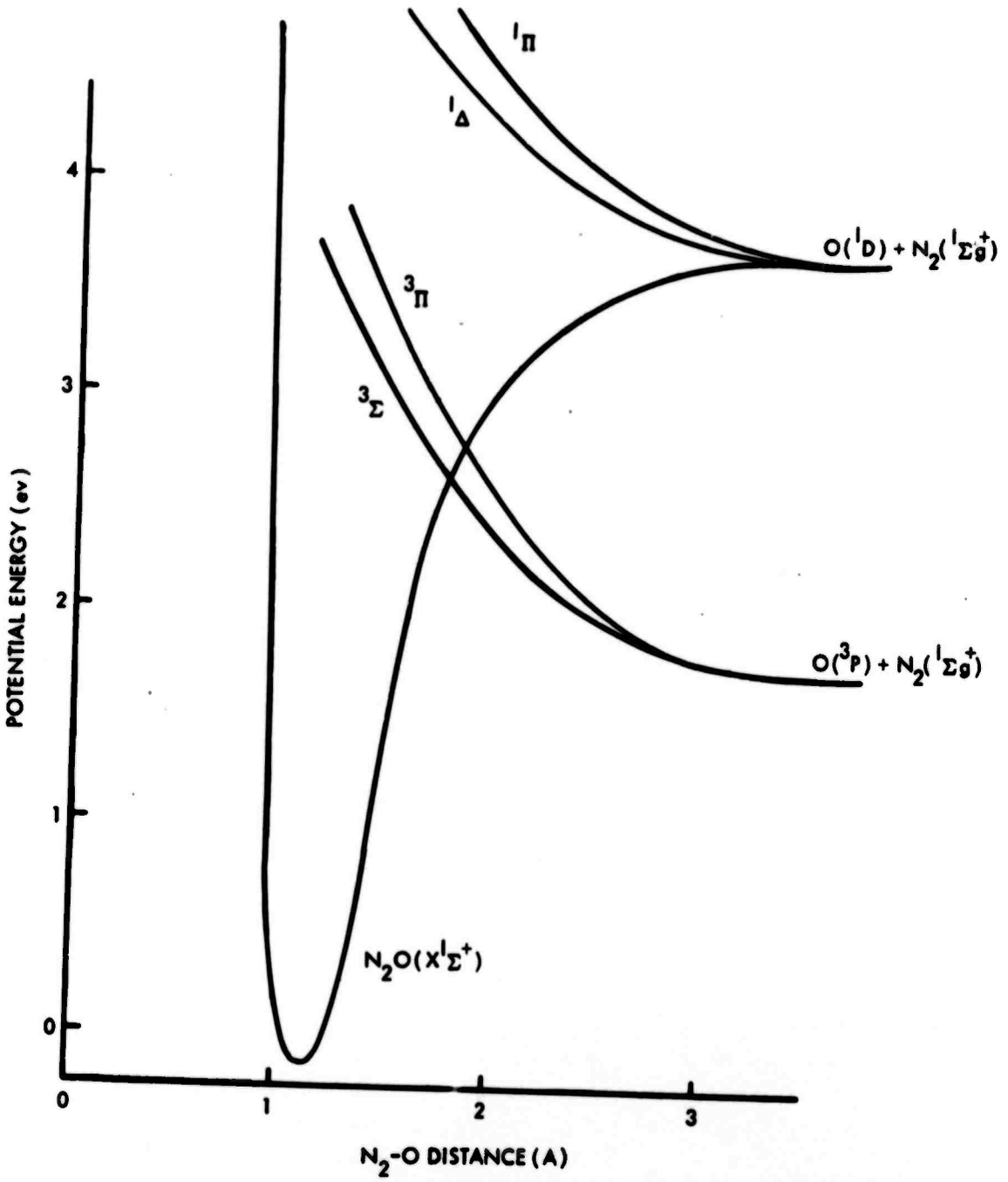

FIGURE 1. Potential Energy Curves for Low-Lying States of the N_2-O System: Collinear Configuration

valence character and thus somewhat less repulsive. The $X^1\Sigma^+$ ground state of N_2O has been characterized by a Morse potential using numerical values from Herzberg (Ref. 15). The activation energy associated with the crossing of the $^1\Sigma^+$ - $^3\Sigma$ curves has been taken from the high-pressure limit of the unimolecular decomposition of $N_2O(X^1\Sigma^+)$ into $O(^3P) + N_2(X^1\Sigma_g^+)$--see Ref. 18. The details of this are presented in Section IV, together with a brief review of pertinent parts of the decomposition reaction. Although it is not possible to give a reliable estimate of the accuracy of most of these potential energy curves, it is unlikely that errors in relevant portions of the crossing region exceed 1 ev, at least for the collinear configuration, $\alpha = 180^\circ$; the decrease in the well depth of the ground state of N_2O with α decreasing from 180° is taken from Peyerimhoff and Buenker (Ref. 16).

For a noncollinear configuration, a twofold degeneracy existing for states other than Σ states is removed, so that each Π, Δ, ... state splits into two states of lower symmetry: for the appropriate point group C_s these are described as A′ and A″, respectively--see Herzberg (Ref. 15), pp. 10, 576. In general, the energies of these different states will vary differently with α, with R(N-N), and with R(N-O); a possible schematic diagram is shown in Fig. 2 (Ref. 19). It must be stressed that the details of Fig. 2 are certainly not correct, but it does show the large number of possible curve crossings whose number and position can vary quite significantly with α, R(N-N), and R(N-O).

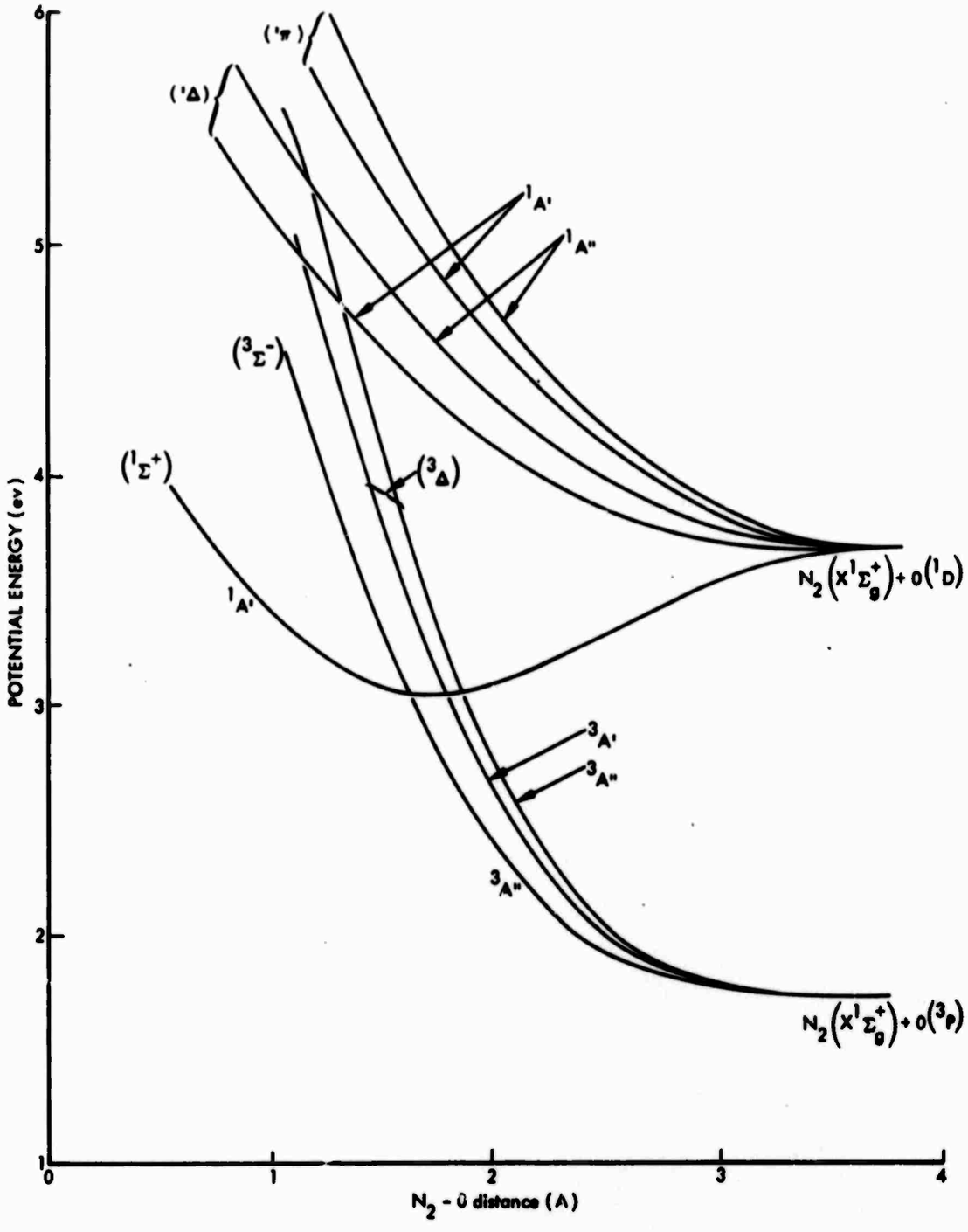

FIGURE 2. Potential Energy Curves for Low-Lying States of the N_2-O System: Bent Configuration, Corresponding to $\alpha = N\text{-}\hat{N}\text{-}O = 120^\circ$. State Assignments are in Parentheses; ($^3\Sigma$), etc., Correspond to the Linear Configuration, $\alpha = 180^\circ$, of Fig. 1.

III. THE CURVE-CROSSING MODEL

A. THE COORDINATE SYSTEM AND THE HAMILTONIAN

Three different modes of motion are considered here: namely, electronic, vibrational, and translational/rotational. These will be described in terms of the coordinates $\underset{\sim}{r}$, $\underset{\sim}{\rho}$, and $\underset{\sim}{R}$, respectively, defined as shown in Fig. 3 (for clarity only one electron is shown). This definition has the advantage that the motion of the center of mass is eliminated, and the kinetic energy terms in the Hamiltonian are separable and are given by the sums of squares of the appropriate momenta. Thus,

$$H^{(o)} = T(\underset{\sim}{r}) + T(\underset{\sim}{\rho}) + T(\underset{\sim}{R}) + V(\underset{\sim}{r}, \underset{\sim}{\rho}, \underset{\sim}{R}) \qquad (6)$$

where $T(\underset{\sim}{q}) = -(\hbar^2/2M)\nabla^2_{\underset{\sim}{q}}$ are the appropriate kinetic energy operators in terms of the proper reduced mass M and the coordinate $\underset{\sim}{q}$ (= $\underset{\sim}{r}$, $\underset{\sim}{\rho}$, $\underset{\sim}{R}$), and the potential energy function $V(\underset{\sim}{r}, \underset{\sim}{\rho}, \underset{\sim}{R})$ involves coupling of all three variables. If the following ansatz for the wave function is made,

$$\Psi^{(o)}_{\lambda} = \varphi_{\lambda}\,(\underset{\sim}{r}; \underset{\sim}{R})\; \chi_{\lambda}(s)\; \theta_{\lambda}\,(\underset{\sim}{\rho}; \underset{\sim}{R})\; f_{\lambda}(\underset{\sim}{R})\;, \qquad (7)$$

where $\varphi_{\lambda}\,(\underset{\sim}{r}; \underset{\sim}{R})$ is the spatial part of the electronic wave function, which depends parametrically on the coordinate $\underset{\sim}{R}$ (dependence on the vibrational coordinate $\underset{\sim}{\rho}$ is ignored); while $\chi_{\lambda}\,(s)$ is the appropriate spin wave function; $\theta_{\lambda}(\underset{\sim}{\rho}; \underset{\sim}{R})$ is the vibrational wave function which again depends parametrically on $\underset{\sim}{R}$; and $f_{\lambda}(\underset{\sim}{R})$ is the translational-rotational wave function, describing the motion of O relative to N_2.

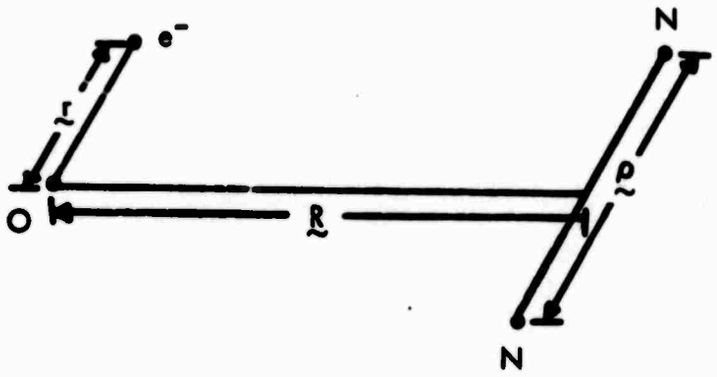

FIGURE 3. The Coordinate System

The curve crossings all involve a change in spin quantum number, so that they arise from the spin-orbit coupling term in the Hamiltonian,

$$H^{SO} = \xi(r)\,(\underset{\sim}{L}\cdot\underset{\sim}{s}) \qquad (8a)$$

$$\xi(r) = (1/2m^2c^2)(1/r)(dV/dr) \sim (Ze^2/2m^2c^2)(1/r^3)\,, \qquad (8b)$$

where $\underset{\sim}{L}$ is the angular momentum operator of the electron and $\underset{\sim}{s}$ is its spin operator, and $V(r) \sim Ze^2/r$ is the central field potential energy.

B. LANDAU-ZENER FORMULA AND TRANSITION MATRIX ELEMENT

Following the characterization of the potential energy curve in Section II, the probability of a diabatic curve crossing must be calculated. For two curves corresponding to states λ, μ which intersect at $R = R_c$, this probability is assumed to be given by the Landau-Zener expression (Ref. 20),

$$P_{\lambda\mu} = \exp\{-\eta_{\lambda\mu}(R_c)\}, \tag{9}$$

where

$$\eta_{\lambda\mu}(R_c) = \frac{2\pi}{u_c \hbar} \left[\frac{|V_{\lambda\mu}(R)|^2}{|(d/dR)(V_{\mu\mu} - V_{\lambda\lambda})|} \right]_{R = R_c} \tag{10}$$

with $u_c = \{2K(R_c)/M\}^{1/2}$ = relative velocity at the crossing point R_c at which the relative kinetic energy is $K(R_c)$.

To determine the transition matrix element at the crossing point, $V_{\lambda\mu}(R_c)$, note that the transition is essentially an electronic one; however, there is the possibility of a change in internuclear separation ρ of the N_2 molecule or more correctly of a change in effective vibrational quantum number of the N-N-O system which corresponds asymptotically to a change in the vibrational quantum number of N_2.

Thus, with the ansatz (8) for the spin-orbit Hamiltonian and the ansatz (7) for the total wave function of the system (from which the translational wave function $f_\lambda(\underset{\sim}{R})$ has to be taken out in order to arrive at the transition matrix element $V_{\lambda\mu}(R_c)$ to be inserted in the Landau-Zener formula), the following equation is found

$$V_{\lambda\mu}(R_c) = \left[\varphi_\lambda(\underset{\sim}{r}; \underset{\sim}{R}) \chi_\lambda(s) \theta_\lambda(\underset{\sim}{\rho}; \underset{\sim}{R}), H^{SO} \varphi_\mu(\underset{\sim}{r}; \underset{\sim}{R}) \chi_\mu(s) \theta_\mu(\underset{\sim}{\rho}; \underset{\sim}{R}) \right]_{R = R_c}$$

$$= V^{el}_{\lambda\mu}(R_c) \left[q^C_{\lambda\mu}(R_c) \right]^{1/2}, \tag{11}$$

where

$$V^{el}{}_{\lambda\mu}(R_c) = \left[\varphi_\lambda(\underset{\sim}{r};\ \underset{\sim}{R}) X_\lambda(s)\ ,\ H^{SO}\ \varphi_\mu(\underset{\sim}{r};\ \underset{\sim}{R}) X_\mu(s) \right]_{R = R_c} \tag{12a}$$

$$q^{C}{}_{\lambda\mu}(R_c) = \left| \left[\theta_\lambda(\varrho;\ \underset{\sim}{R}),\ \theta_\mu(\varrho;\underset{\sim}{R}) \right]_{R = R_c} \right|^2 . \tag{12b}$$

In other words, the transition matrix element is the product of an electronic transition matrix element $V^{el}{}_{\lambda\mu}$ multiplied by a vibrational overlap integral (written as the square root of a "collision-modified Franck-Condon factor"), both evaluated at the crossing point.

To lowest order,

$$V^{el}{}_{\lambda\mu}(R_c) \simeq V^{el}{}_{\lambda\mu}(R \to \infty) = V^{el}\left\{O(^1D_2 - {}^3P_2)\right\} \tag{13a}$$

for the electronic transition matrix element, and for the isolated oxygen alone, Yamanouchi and Horie (Ref. 21) give the result,

$$V^{el}\ O(^1D_2 - {}^2P_2) \simeq 80\ cm^{-1} . \tag{13b}$$

Accordingly, one would expect the transition matrix element between the $^1\Sigma^+$ and triplet curves to be of this order (Ref. 19). To obtain detailed numerical values of the transition matrix elements would be a major computational problem, and thus our approach has been to use various experimental data to obtain plausible empirical values for V^{el}, which is treated as a parameter. This point is discussed further in Sections IV and VII.

C. THE COLLISION-MODIFIED FRANCK-CONDON FACTOR q^C

To the approximation of Eq. (11), the effect of the vibration on the transition matrix element enters solely through the vibrational

overlap integral and is customarily expressed in terms of its mean square, the collision-modified Franck-Condon factor $q^C_{\lambda\mu}(R)$ of Eq. (12b). In the limit of infinite internuclear separation R, $q^C_{\lambda\mu}(R)$ becomes just the ordinary Franck-Condon factor $q_{\lambda\mu}$

$$q^C{}_{\lambda\mu}(R \to \infty) \equiv q_{\lambda\mu} = \left| \left[\theta_\lambda(\underset{\sim}{\rho}),\ \theta_\mu(\underset{\sim}{\rho}) \right] \right|^2 \tag{14}$$

Here $\theta_\lambda(\underset{\sim}{\rho})$ is the vibrational wave function for an isolated N_2 molecule and thus the Franck-Condon factor $q_{\lambda\mu}$ is just a Kronecker δ;

$$q_{\lambda\mu} = \begin{cases} 1 \text{ if } v_\lambda = v_\mu \\ 0 \text{ if } v_\lambda \neq v_\mu \end{cases} \tag{15}$$

where v_λ, v_μ are the vibrational quantum of N_2 in states λ, μ.

To obtain an estimate for the possible vibrational excitation or de-excitation in curve-crossing collisions using the present model, we have to go beyond the approximation of $q_{\lambda\mu}$, and in fact the previous work of Nikitin (Ref. 22) and Bauer (Ref. 23) is extended here.

Because of the considerable difference in the interaction of N_2 with $O(^1D)$ and $O(^3P)$, as shown in Figs. 1 and 2, one would expect that the collisional distortion of the vibrational motion will be different for the two states, (which we will now call s and t for "singlet" and "triplet," respectively, rather than λ and μ) consequently, there may be a vibrational overlap between adjacent vibrational levels in N_2O which correspond asymptotically to adjacent vibrational levels of N_2.

Using first-order perturbation theory for the vibrational wave function $\theta_\lambda(\underset{\sim}{\rho}; \underset{\sim}{R})$ of Eq. (7),

$$\theta_{\lambda i}(\underset{\sim}{\rho};\underset{\sim}{R}) = \theta_{\lambda i}(\underset{\sim}{\rho}) + \sum_{k \neq i} \frac{(i|V^*|k)}{E_i - E_k}\ \theta_{\lambda k}(\underset{\sim}{\rho}) , \tag{16}$$

where

$$\theta_{\lambda i}(\underset{\sim}{\rho}) = \lim_{R \to \infty} \theta_{\lambda i}(\underset{\sim}{\rho}; \underset{\sim}{R})$$

is the wave function for vibrational quantum number v_i of N_2; evidently there is no dependence of $\lambda(= s,t)$ in the asymptotic limit.

$$V^* = V^{(\text{singlet})} \text{ or } V^{(\text{triplet})}$$

represents the collisional perturbation of $O^{(s \text{ or } t)}$ on N_2, as a function of $\underset{\sim}{\rho}$ and $\underset{\sim}{R}$.

Inserting the perturbation ansatz of Eq. (16) in the definition, Eq. (12b), of q^C,

$$\left[q^C_{st;\, ij}(R)\right]^{1/2} = \int \theta_{si}(\underset{\sim}{\rho}; \underset{\sim}{R})\, \theta_{tj}(\underset{\sim}{\rho}; \underset{\sim}{R}) d\underset{\sim}{\rho} \sim \int \theta_{si}(\underset{\sim}{\rho})\, \theta_{tj}(\underset{\sim}{\rho}) d\underset{\sim}{\rho} +$$

$$\sum_{k \neq i} \frac{(i|V^s|k)}{E_i - E_k} \int \theta_{tj}(\underset{\sim}{\rho}) \theta_{sk}(\underset{\sim}{\rho}) d\underset{\sim}{\rho} + \sum_{\ell \neq j} \frac{(j|V^t|\ell)}{E_j - E_\ell} \int \theta_{si}(\underset{\sim}{\rho}) \theta_{t\ell}(\underset{\sim}{\rho}) d\underset{\sim}{\rho}. \quad (17)$$

If the collisional perturbation V^* is assumed to be linear in the vibrational coordinate ρ, the relations

$$V^s = a_s(\rho - \rho_e)\, U^s(R) \quad (18a)$$

$$V^t = a_s(\rho - \rho_e)\, U^t(R) \quad (18b)$$

follow for V^*, and to lowest order

$$\left[q^C_{st;\, ii}(R)\right]^{1/2} = \int \theta_i \theta_i \, d\underset{\sim}{\rho} = 1 \quad (19a)$$

$$\left[q_{st;\, ij}(R)\right]^{1/2}_{(i \neq j)} = \frac{a_t\, U^t(R) - a_s\, U^s(R)}{E_i - E_j} (i|\rho|j) \quad (19b)$$

If it is further assumed that $\theta_i(\rho)$ can be described by harmonic oscillator wave functions so that only adjacent levels couple, $(i|\rho|i-1) = \sqrt{i\hbar/2\mu\omega}$, where μ = reduced mass of N_2 and ω = vibrational (angular) frequency, so that

$$\left[q^C_{st;\ i,\ i-1}(R)\right]^{1/2} = \left[a_t\, U^t(R) - a_s\, U^s(R)\right]\sqrt{i/2\mu\hbar\omega^3} \qquad (20)$$

The harmonic oscillator matrix element can be easily evaluated for N_2 to give

$$\sqrt{i/2\mu\hbar\omega^3} = \sqrt{i}/(2.05 \times 10^{-3})\ \text{cm/erg}, \qquad (21)$$

while the triplet parameters can be estimated from the results of O-N scattering (Ref. 24) to give $a_t = 2.65\text{A}^{-1}$ and for an O-N distance of 1.8Å (See Fig. 1), $U^t \cong 1.5$ ev so that

$$a_t U^t(R \simeq 1.8\ \text{A}) = 6.4 \times 10^{-4}\ \text{erg/cm} . \qquad (22)$$

If it is reasonable to assume that the singlet interaction is some fraction of the triplet, say K, then

$$\left[q^C_{st;\ 1,\ 0}(R)\right]^{1/2} = (1 - K)(0.31) \qquad (23)$$

For the numerical calculations that follow, K is varied from 0.8 to 0.2. As a reference for discussion, K = 0.6 is taken as being representative, thus

$$\left[q^C_{st;\ 1,\ 0}(R)\right]^{1/2} \approx 0.124 \qquad (24)$$

Clearly, improvements in this number may be made, but Eq. (24) is expected to be roughly representative for the qualitative treatment which follows. The results for other values of K are given in Appendix A.

IV. UNIMOLECULAR DECOMPOSITION OF N_2O

The nonadiabatic thermal decomposition of N_2O ($^1\Sigma$) has been the subject of many investigations (Refs. 25, 26, and 27). Two experimental facts that emerge from these investigations, in the high-pressure limit, relate to this curve-crossing model. The first fact is the activation energy associated with the decomposition reaction of Eq. (3),

$$N_2O(X^1\Sigma^+) \rightarrow N_2(X^1\Sigma_g^+) + O(^3P) \qquad (3)$$

which is found to be 60 kcal/mole (≃ 2.6 ev). The second is the fact that the pre-exponential factor in the high-pressure rate coefficient is from one to two orders of magnitude smaller than the expected gas kinetic value. Both of these results can be qualitatively explained through the curve-crossing model outlined in the previous sections. The measured activation energy gives insight into the position of the singlet and triplet crossing point--representing the most probable exit channel for the decomposition. It is not entirely clear whether the decomposition reaction occurs primarily through a stretching vibration, giving insight into the collinear configuration case, or whether the decomposition involves a combination of stretching and bending modes. The latter case might be more important because of its larger statistical weight; thus, the measured activation energy presumably provides some angle-averaged minimum singlet-triplet crossing energy.

The low pre-exponential factors can be explained by the spin change required between products and reactants, i.e., a change from the singlet reactant configuration to the triplet product configuration via a direct curve crossing (Ref. 26). On the assumption that

this crossing can be characterized by the Landau-Zener formula, the spin-orbit interaction necessary to explain the low pre-exponential factor is of the order of 200 cm^{-1}. This value is roughly consistent with the value necessary to correlate the measured quenching rate coefficient data on $O(^1D)$ by N_2 and also to explain the efficiency of $O(^3P)$ in relaxing vibrational energy in N_2. These subjects are the content of the next two sections.

V. QUENCHING OF $O(^1D)$ BY N_2

Having established that a direct curve crossing exists between the singlet reactant curves and the triplet product curves as shown in Figs. 1 and 2, an estimate is now developed of the magnitude of the quenching cross section and the likelihood of vibrational energy being channeled into the product N_2. To accomplish this estimate, the potential curves as shown in Figs. 1 and 2 are expanded to include the vibrational structure of both reactant and product N_2 molecules. These molecular curves are shown in Figs. 4 and 5 for the collinear and 120° configuration cases.

In order to perform the quenching calculation, it is assumed, as in earlier calculations (Ref. 1), that the curve-crossing probability at each intersection point is characterized by the Landau-Zener equation, i.e., Eq. (3). The effective force terms in the denominator of η--see Eq. (10)--have been estimated directly from the slopes at the curve-crossing intersection points as shown in Figs. 4 and 5. The values used are given in Table 1.

The collision-modified vibrational overlap at each crossing point, as outlined in Section IIIC, has been assumed for calculational purposes to be $\left(q^C\right)^{\frac{1}{2}} = 0.124$ which results when the singlet interaction, $a_s U^s$, is assumed to be 60% of the triplet interaction, as shown in Eq. (24). The results for other assumed values are given in Appendix A.

The electronic part of the interaction matrix element at each crossing point (the spin-orbit interaction) has been treated as a parameter of the order of magnitude given for the isolated $O(^3P)$ and $O(^1D)$, as discussed in Section IIIB--see Eq. (13b)--and also by the results of the unimolecular decomposition measurements.

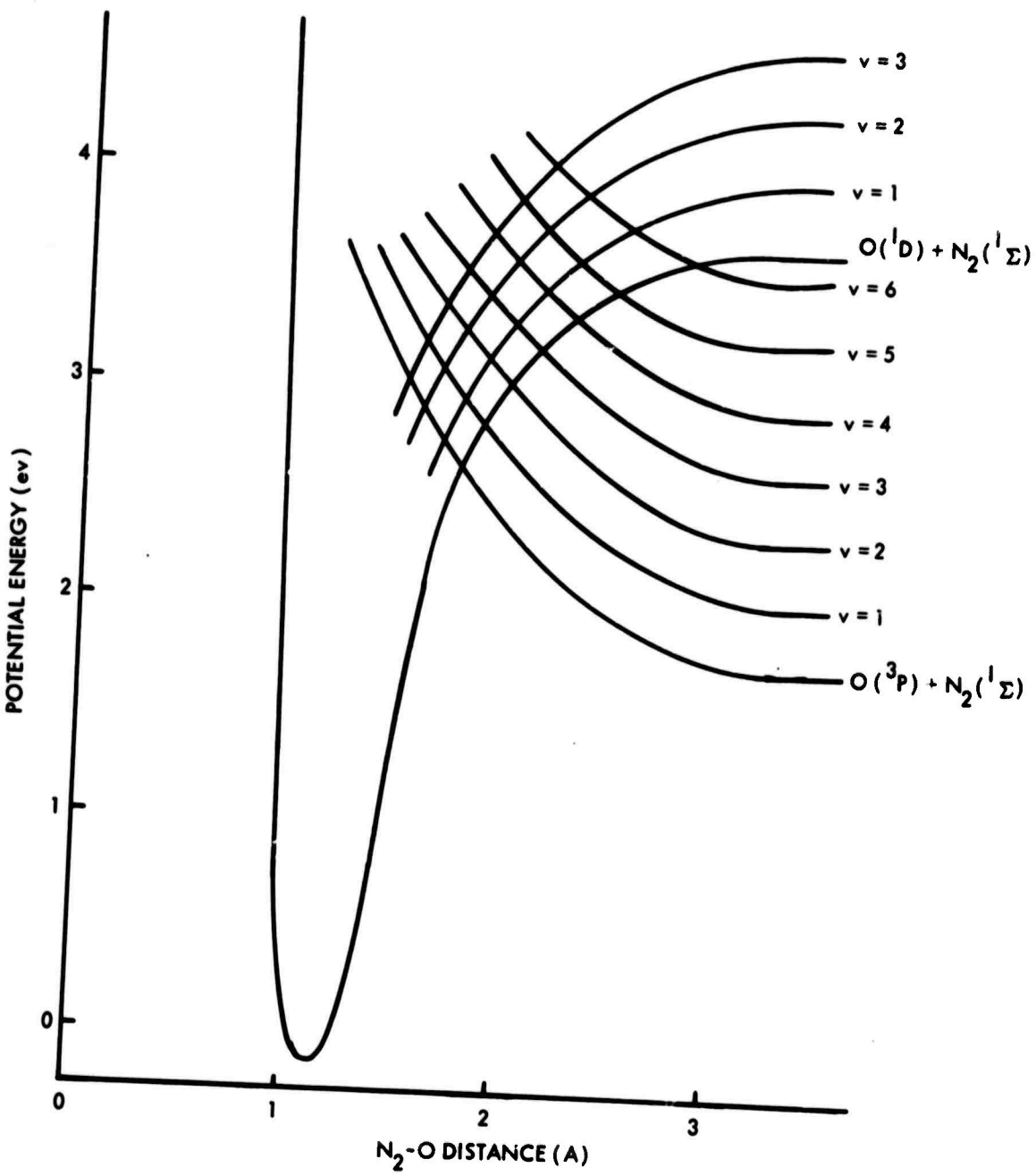

FIGURE 4. Schematic Potential Energy Curves of the N_2-O System, for Vibrational-Electronic Coupling: Collinear Configuration

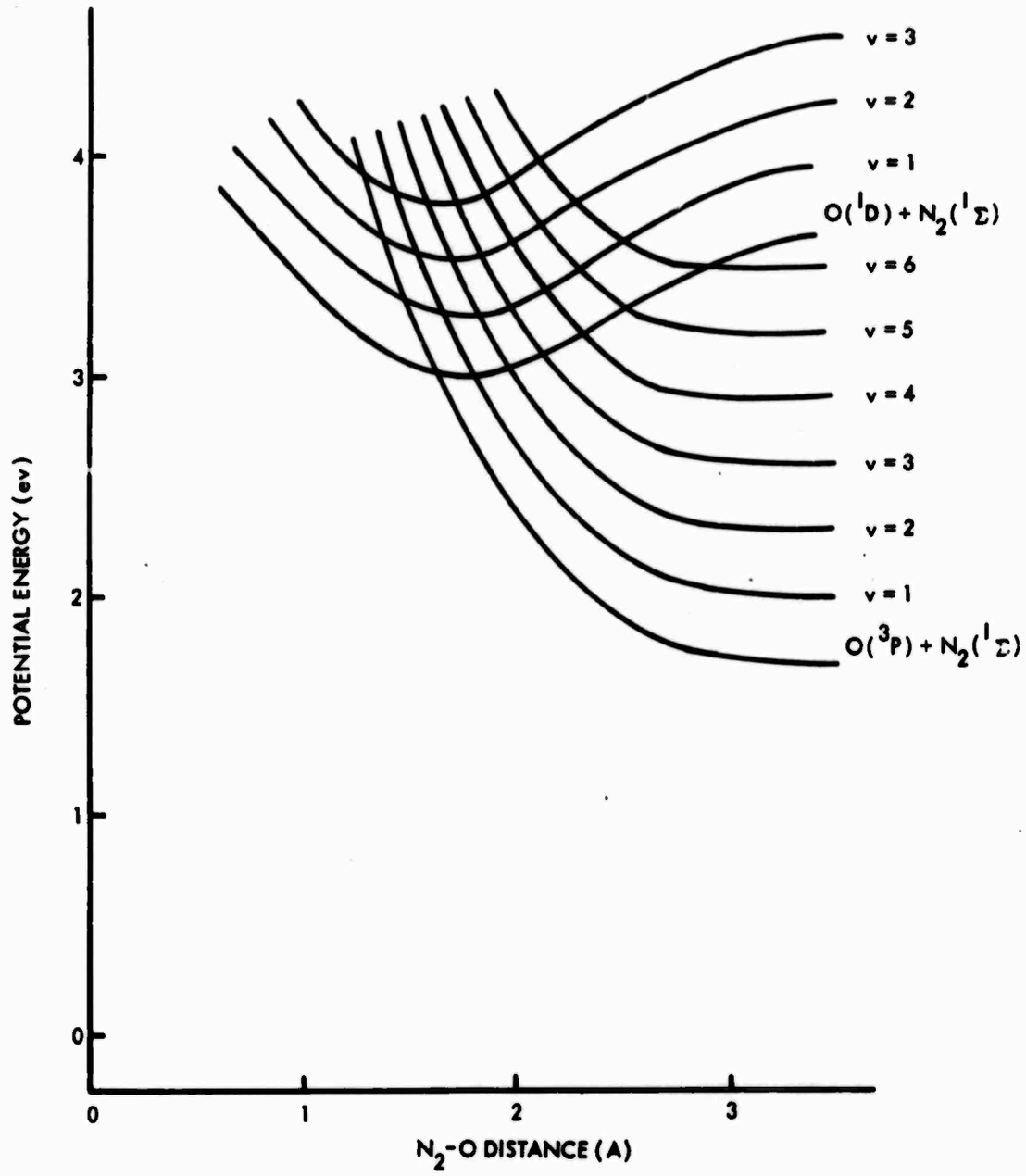

FIGURE 5. Schematic Potential Energy Curves for the N_2-O System, for Vibrational-Electronic Coupling: Bent Configuration, Corresponding to $\alpha = N\text{-}\hat{N}\text{-}O = 120^\circ$

TABLE 1. EFFECTIVE FORCE TERMS USED IN THE QUENCHING OF $O(^1D)$ BY N_2

Triplet Vibrational Level	Collinear Case, ev/A	120° Case, ev/A
6	0.7	0.65
5	1.29	1.03
4	1.8	1.26
3	2.0	1.5
2	2.6	1.54
1	2.92	1.58
0	4.28	1.5

Following the definition of the curve-crossing probability at each intersection point as outlined above, a classical diffusion calculation has been performed as a function of relative kinetic energy. The details of this diffusion calculation have been presented elsewhere (Refs. 1 and 28).

The results for the partial quenching cross sections for the collinear and the 120° configuration cases are shown in Tables 2 and 3, respectively.* For these calculations the effective force terms listed in Table 1 have been used. As pointed out in Section IV, the singlet-triplet crossing point was established from the 60 kcal/mole activation energy determined in unimolecular decomposition

*All of these cross sections refer to the collision partners $N_2(X^1\Sigma_g^+)$ and $O(^1D)$ entering along the lowest possible potential energy curve, i.e., the $^1\Sigma^+$ curve of Fig. 1 or the $^1A'$ curve of Fig. 2. Thus, the total cross sections must be multiplied by the statistical weight factor $g \geq 0.2$--see discussion below Eq. (25).

TABLE 2. PARTIAL QUENCHING CROSS SECTIONS FOR $O(^1D) + N_2$ REACTION (IN 10^{-16} CM^2)*

COLLINEAR CONFIGURATION

Vibrational Level \ V_{el}**	100 cm^{-1}	300	500
6	0.0	0.0	0.0
5	0.0	0.0	0.0
4	0.0	0.0	0.0
3	0.0	0.0	0.0
2	0.0	0.0	0.0
1	0.0	0.0	0.12
0	0.41	3.33	7.57
Total Quenching Cross Section	0.41	3.33	7.69

*Franck Condon Factor = 0.015 (Corresponds to K = 0.6 in Eq. 23).
Relative kinetic energy = 0.1 ev.

**Assumed spin-orbit interaction.

TABLE 3. PARTIAL QUENCHING CROSS SECTIONS FOR $O(^1D) + N_2$ REACTION (IN $10^{-16}CM^2$)*

BENT (120°) CONFIGURATION

Vibrational Level \ V_{el}**	100 cm^{-1}	300	500
6	0.0	0.0	0.0
5	0.0	0.0	0.0
4	0.0	0.0	0.0
3	0.0	0.0	0.0
2	0.0	0.0	0.02
1	0.0	0.03	0.66
0	1.54	9.42	12.20
Total Quenching Cross Section	1.54	9.45	12.88

*Franck Condon Factor = 0.015 (Corresponds to K = 0.6 in Eq. 23).
Relative kinetic energy = 0.1 ev.

**Assumed spin-orbit interaction.

measurements. The curves shown in Figs. 4 and 5 are based on this value, i.e., the energy separation from the minimum well depth of the N_2O molecule to the crossing of the v = 0 singlet and triplet curves, and the effective force terms shown in Table 1 have been estimated from these figures. It is unlikely, however, that the unimolecular decomposition products are vibrationally unexcited because the transition probably passes through a vibrationally excited intermediate state. Therefore the measured activation energy probably represents the energy separation between the minimum N_2O well depth and some excited vibrational level of the triplet curve. The net effect of this would be to reduce the effective force terms at each crossing point from those given in Table 1. In order to test the effect of this on the partial quenching cross sections, the effective force terms shown in Table 1 have been arbitrarily reduced by 30% and the quenching calculation repeated for both the collinear and 120° configuration cases. The results for these calculations are given in Tables 4 and 5.*

Several features of these results are of importance:

a. The total quenching cross section increases with the magnitude of the assumed spin-orbit interaction.
b. The total quenching cross section is larger for the 120° case than for the collinear, as expected from the reduced effective force terms for the bent configuration geometry.
c. The quenching cross sections are only weakly dependent on collision energy due to the attractive nature of the interaction potential for the reactants.
d. The interaction matrix element necessary to give rough agreement with experimental quenching measurements is

*All of these cross sections refer to the collision partners $N_2(X\,^1\Sigma_g^+)$ and $O(^1D)$ entering along the lowest possible potential energy curve, i.e., the $^1\Sigma^+$ curve of Fig. 1 or the $^1A'$ curve of Fig. 2. Thus, the total cross sections must be multiplied by the statistical weight factor $g \geq 0.2$--see discussion below Eq. (25).

TABLE 4. PARTIAL QUENCHING CROSS SECTIONS FOR $O(^1D) + N_2$ REACTION (IN 10^{-16} CM^2)*
COLLINEAR CONFIGURATIONS**

Vibrational Level \ V_{el}***	100 cm^{-1}	300	500
6	0.0	0.0	0.0
5	0.0	0.0	0.0
4	0.0	0.0	0.0
3	0.0	0.0	0.0
2	0.0	0.0	0.0
1	0.0	0.0	0.21
0	0.58	4.54	9.44
Total Quenching Cross Section	0.58	4.54	9.65

*Franck Condon Factor = 0.015 (Corresponds to K = 0.6 in Eq. 23)
Relative kinetic energy = 0.1 ev.
**0.7 times effective force terms shown in Table 1.
***Assumed spin-orbit interaction.

TABLE 5. PARTIAL QUENCHING CROSS SECTIONS FOR $O(^1D) + N_2$ REACTION (IN 10^{-16} cm^2)*
BENT (120^o) CONFIGURATION**

Vibrational Level \ V_{el}***	100 cm^{-1}	300	500
6	0.0	0.0	0.0
5	0.0	0.0	0.0
4	0.0	0.0	0.0
3	0.0	0.0	0.0
2	0.0	0.01	0.03
1	0.0	0.23	1.22
0	2.16	11.14	10.64
Total Quenching Cross Section	2.16	11.38	11.89

*Franck Condon Factor = 0.015 (Corresponds to K = 0.6 in Eq. 23).
Relative kinetic energy = 0.1 ev.
**0.7 times the effective force listed in Table 1.
***Assumed spin-orbit interaction.

consistent with the unimolecular decomposition calculation presented in the previous section, but this value is significantly larger than the spin-orbit interaction energy for an isolated oxygen atom (cf. Ref. 21).

e. Due to the small vibrational overlap between adjacent vibrational levels, the partial cross sections for exciting N_2 vibrational levels, $v > 0$, is small; and the fraction of collisions leading to the $v \geq 1$ exit channel is of the order of 0.10 or smaller (note that the fraction of energy which channels into excited vibrational levels of N_2 is roughly $(0.1)(1/7) \lesssim 2\%$).

Here the effective de-excitation cross section, σ_d, has been estimated and found to be only weakly dependent on velocity u (or temperature T). The expression for the de-excitation rate constant $k_d(T)$ is

$$k_d(T) = g \int \sigma_d(u)\, f(u,T)\, du, \tag{25a}$$

where f(u, T) is the (Maxwell-Boltzmann) velocity distribution function and g is a statistical weight factor; because σ_d is only weakly dependent on u, $k_d(T)$ may be reduced to the following:

$$k_d(T) = g\, \overline{\sigma_d}\, \overline{u(T)} \tag{25b}$$

where $\overline{u(T)}$ is the thermal mean speed $\simeq 8 \times 10^4$ cm/sec at $T = 300^{\circ}K$.

The statistical weight factor, g, is the probability that the $O(^1D)$ atom approaches the N_2 molecule in the configuration corresponding to a crossing. For the collinear case (cf. Fig. 1), this corresponds to the $^1\Sigma$ state rather than the $^1\Delta$ or $^1\Pi$, i.e., $g = 1/(1 + 2 + 2) = 1/5$. For noncollinear configurations, the statistical factor is uncertain, since additional curve crossings may take place, involving the two repulsive states. Thus, using $g = 0.2$ (which may be an underestimate) and $u(T) = 8 \times 10^4$ cm/sec, the range of experimental values of $k_d(T)$,

which is (4-9) x 10^{-11} cm^3/sec (Ref. 13), corresponds to $\bar{\sigma}_d$ = (2.5 - 5.6) x 10^{-15} cm^2, or two to six times the calculated value of the cross section. In fact, the lower experimental value is more plausible, and agreement with experiment within a factor 2-3 is certainly all that can be expected by a calculation as primitive as the present one.

VI. N_2 VIBRATIONAL RELAXATION BY $O(^3P)$ ATOMS

The results of the previous two sections can be used to calculate the vibrational relaxation cross sections for N_2 by O atoms by analogy to the curve-crossing model for the relaxation of N_2 by alkali atoms (Ref. 3). For an estimate of this process, refer to Fig. 4, the collinear interaction of $O(^3P)$ atoms with $N_2(^1\Sigma_g^+)$, i.e., reaction (5).

As can be seen from this figure, this mechanism for atom relaxation is accompanied by an activation energy of about 0.8 ev from the reactants to the first crossing point of the v = 0 singlet surface. The activation energy associated with this collinear crossing configuration will be considerably lower than for noncollinear configurations due to the decrease in the well depth of the N_2O singlet surface for angles less than 180°. It should be remarked, however, that since the unimolecular decomposition of N_2O may preferentially give vibrationally excited N_2, an activation energy of 0.8 ev is likely to be a maximum value.

The probability of transition from the v = 1 reactant surface to the v = 0 product surface, P, is roughly given by $2P_a(1 - P_b)(1 - P_a)$, where P_a and P_b are the diabatic (i.e., curve-crossing) probabilities at the $v_t = 0$, $v_s = 0$ and $v_t = 1$, $v_s = 0$, intersections, respectively. The probabilities will be considerably larger than in the corresponding quenching case since the velocity at the crossing points will be small by comparison. Very crudely, the vibrational deactivation probability may be taken as the ratio of the v = 1 to v = 0 partial quenching cross sections since the increased probabilities due to a considerably lower velocity at the crossing point will be counteracted by the additional adiabatic curve crossing necessary to transfer from the v = 1 reactant surface to the v = 0 singlet surface.

For the assumed range of spin-orbit interaction values, the ratio of the $v = 1$ to $v = 0$ cross sections is roughly 0.1. The relaxation rate coefficient is thus

$$P_{10} = spe^{-E_{act}/kT}, \tag{26}$$

where

s = steric factor to account for noncollinear configurations
$\simeq 1/6$

p = collisional deactivation probability/collision

$$\simeq \frac{\sigma(v = 1)}{\sigma(v = 0)} \simeq 0.1$$

and

E_{act} = activation energy to reach first curve crossing
$\simeq 0.8$ ev.

This numerical value for the collisional deactivation probability per collision is confirmed by more detailed calculations but is clearly sensitive to the vibrational overlap and the assumed spin-orbit interaction at the crossing points, as in the quenching case. The important point is that the temperature dependence is weak in the pre-exponential factor and should mainly come from the activation energy term. Inserting the above numbers into Eq. (26), we get

$$P_{10} = 1.7 \times 10^{-2} \exp\{-9.5 \times 10^3/T(^oK)\} . \tag{27}$$

In order to compare this value with the available experimental data, the probability can be converted to a relaxation time, τ, by

$$\frac{1}{\tau} = P_{10} Z\left[1 - e^{-hc\omega/kT}\right], \tag{28}$$

where Z = collision frequency

$$= \left(\frac{8\pi kT}{\mu}\right)^{1/2} \sigma^2 N_B$$

ω = vibrational spacing

N_B = number density

and τ = relaxation time

Using $\sigma = 3.02$ A, we get

$$P\tau_{4000^\circ K} = 0.7\ \mu \text{ sec atm}$$

and

$$P\tau_{3000^\circ K} = 1.1\ \mu \text{ sec atm}$$

where P is the pressure (in atmospheres).

Figure 6 shows the calculated relaxation time for the relaxation of N_2 vibrational energy in collisions with O atoms as compared with available data. For extrapolation to other temperatures, the equation of the calculated relaxation time is (T in $^\circ$K, P in atm, τ in sec)

$$(1/P\tau) = 1.64 \times 10^9\ T^{-1/2}\ e^{-9500/T}\ [1 - e^{-3250/T}] \qquad (29)$$

It must be stressed that the "non-adiabatic" or "chemical" mechanism for the vibrational relaxation of N_2 by O that has been discussed here is not the only one. There is also the "adiabatic" or "Landau-Teller" mechanism--cf. Ref. 29. Using the semi-empirical model of Millikan and White (Ref. 30) for the Landau-Teller mechanism, we find that

$$(P\tau)_{\substack{\text{chem} \\ \text{(see Eq. 29)}}} < (P\tau)_{\text{Landau-Teller}} \text{ for } T \gtrsim 600^\circ K\ . \qquad (30)$$

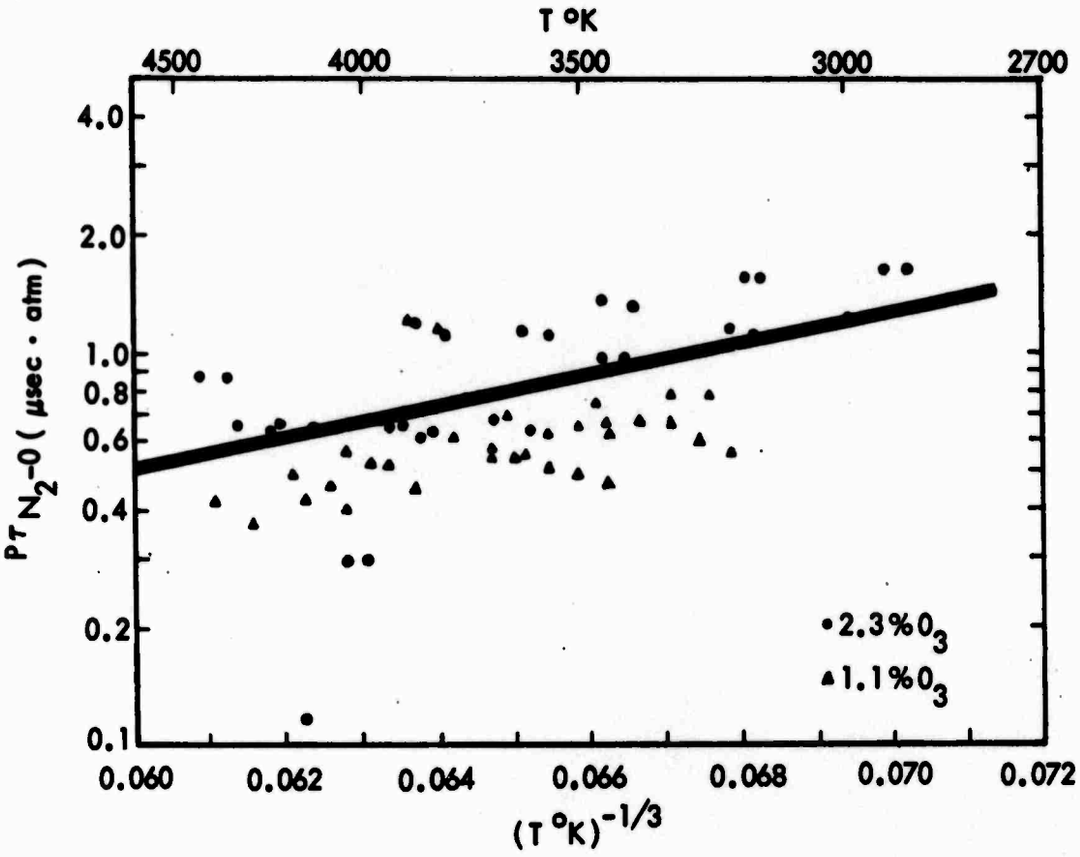

FIGURE 6. Vibrational Relaxation of N_2 by Collision with O. The Theoretical Curve of Eq. (29) is Superposed on the Experimental Data of Breshears and Bird (Ref. 14).

In other words, for $T \gtrsim 600^{\circ}K$ the chemical mechanism dominates, while for $T \lesssim 600^{\circ}K$ the 0.8 ev activation energy for the chemical mechanism presents such a big barrier that the nonchemical Landau-Teller mechanism dominates. In fact, a comparable situation is known to occur for NO-NO collisions--see Refs. 22 and 31.

VII. DISCUSSION

From the results of the previous sections, several features of the various processes--in particular of the quenching reaction (4)--can be indicated.

1. It may seem surprising that the general order of magnitude of these rather large cross sections [~ (1/10) gas kinetic] can be explained by the small interaction $V^{el} \sim 100\text{-}500\ cm^{-1}$ (0.01 - 0.04 ev) associated with the spin-change transition. This follows immediately from the assumption of a Landau-Zener transition, i.e., on interactions occurring over relatively small distances and calculable by perturbation theory. There is the possibility that these assumptions are inadequate, so that "close-coupling" effects may be important. It should be noted that close-coupling calculations for a problem as complex as the present one are hardly feasible at present; nor are they likely to become feasible in less than three to five years.

2. The vibration-electronic coupling in this reaction appears to be very small. This result is a direct consequence of the small overlap between adjacent vibrational levels even in the collisionally perturbed case. Although the estimate of the modified Franck-Condon factor is crude, it is rather unlikely that, even with a more adequate estimate of the vibrational overlap, a significant overlap between vibrational levels separated by more than one quantum will be predicted. This point is made even stronger by the relatively large cross sections predicted for the $v = 0$ channel, i.e., no vibrational excitation. It is anticipated that other quenching reactions which proceed entirely via the crossing of covalent potential energy curves will show similar behavior. This conclusion is in marked contrast to the results of quenching via ionic intermediate complexes where the vibration-electronic coupling is large.

3. In the calculations presented here only one of the triplet curves (see Fig. 1) was included explicitly. Inclusion of the second curve could increase the interaction matrix element for crossing points greater than the v = 0 level; however, there appears to be no adequate way of accounting for the interaction at the intersection of three potential energy curves.

In addition, the position of the crossing point of the v = 0 singlet and triplet curves was established by the activation energy of the high-pressure unimolecular decomposition of N_2O, as discussed in Section IV. It is likely that this activation energy would be more representative of a higher lying vibrational level, e.g., the intersection of the v = 3 singlet and triplet curves, and thus the actual effective force terms given in Table 1 would be reduced with a corresponding increase in the adiabatic curve-crossing character and hence total quenching cross sections.

This conclusion is verified by the calculations based upon 0.7 times the effective force terms as given in Table 1.

4. The maximum contribution to the total quenching cross section appears to come from noncollinear configuration trajectories. This conclusion is a result of the reduction in the effective force evident at the curve-crossing points due to the decrease in the singlet well depth with decreasing angle $\alpha = N - \hat{N} - O$ from 180°. As a consequence of this reduction, the N_2 quenching product is likely to be rotationally excited following a successful quenching reaction.

The degree of rotational excitation may be estimated as follows. For an N-N internuclear distance r_e, the effective impact parameter b of the collision is

$$b = \tfrac{1}{2} r_e \sin(\pi - \alpha) \qquad (30a)$$

For incident velocity u, the initial angular momentum available for transfer to rotation is $M_{O;N_2}$ ub corresponding to a maximum rotational quantum number

$$J_{max} = M_{O;N_2} ub/\hbar \qquad (30b)$$

where

$$M_{O;N_2} = M_O M_{N_2}/(M_O + M_{N_2}) = 1.69 \times 10^{-23} \text{ gm.}$$

Using $u = 4.5 \times 10^5$ cm/sec (corresponding to a kinetic energy of 1 ev, which is appropriate at the crossing point--see Figs. 1 and 2) and $b = 0.5 \times 10^{-8}$ cm gives $J_{max} = 35$, so that $E_{rot,\,max} = B_e J(J+1) \simeq 0.31$ ev; thus, at most 15 percent of the excitation energy (= 2 ev) can go into rotation.

In summary, on the basis of qualitative features of the potential energy surfaces for the quenching of $O(^1D)$ by N_2, less than 5 percent of the electronic quantum of $O(^1D)$ is expected to channel into the vibrational levels of N_2. Thus, reaction (2) will not be a significant source of vibrational energy in the upper atmosphere. In addition, the relaxation of N_2 vibrational energy by $O(^3P)$ atoms at high temperatures is consistent with this curve-crossing model and suggests a strong temperature dependence for extrapolation to lower temperatures appropriate to upper atmospheric conditions. Note, however, that below about 600°K the effect of "adiabatic" or "Landau-Teller" vibrational relaxation of N_2 by O is likely to predominate over the present "chemical" mechanism.

REFERENCES

1. E. Bauer, E. R. Fisher and F. R. Gilmore, J. Chem. Phys., 51, 4173 (1969). "De-excitation of Electronically Excited Sodium by Nitrogen."
2. E. R. Fisher and G. K. Smith, Applied Optics, 10, 1803 (1971). "Vibration-Electronic Coupling in the Quenching of Electronically Excited Alkali Atoms by Diatomics."
3. E. F. Fisher and G. K. Smith, Phys. Letters, 6, 438 (1970). "Vibrational Relaxation of N_2 by Metal Atoms."
4. The model of an ionic intermediate state as presented in the above-mentioned work is somewhat oversimplified; for a discussion of the actual potential energy curves in which the ionic character is strongly displayed, cf. M. Krauss, J. Res. NBS, 72A, 553 (1968). "Interaction Energy Surfaces for Li(2^2S) and Li(2^2P) with H_2."
5. A related process which involves higher lying excited states of N_2O and thus is not considered here is the following:

$$N + NO \rightarrow N_2(v) + O$$

6. D. R. Bates and B. L. Moiseiwitsch, Proc. Phys. Soc., A67, 805 (1954). "Inelastic Heavy Particle Collisions Involving the Crossing of Potential Energy Curves-I."
7. J. B. Hasted and A. Y. J. Chong, Proc. Phys. Soc., A80, 441 (1962). "Electron Capture Processes for Multiply Charged Ions."
8. R. E. Olson, F. T. Smith and E. Bauer, Appl. Opt. 10, 1848 (1971). "Estimation of the Coupling Matrix Elements for One-Electron Transfer Systems."

9. M. Krauss, Ann. Rev. Phys. Chem., 21, 39 (1970). "Potential Energy Surfaces."

10. J. C. G. Walker, R. S. Stolarski, A. F. Nagy, Ann. de Geophys. 25, 831 (1969). "The Vibrational Temperature of Nitrogen in the Thermosphere."

11. E. Bauer, R. H. Kummler, and M. H. Bortner, Appl. Opt. 10, 1861 (1971). "Internal Energy Balance and Energy Transfer in the Lower Thermosphere."

12. E. C. Zipf, Canad. J. Chem., 47, 1863 (1969). "Deactivation of Excited States."

13a. R. A. Young, G. Black and T. G. Slanger, J. Chem. Phys., 49, 4758 (1968), "Reaction and Deactivation of $O(^1D)$."

13b. J. F. Noxon, J. Chem. Phys., 52, 1852 (1970). "Optical Emission from $O(^1D)$ and $O_2(b^1\Sigma_g)$ in UV Photolysis of O_2 and CO_2."

13c. M. Loewenstein, J. Chem. Phys., 54, 2282 (1971). "Relative Quenching Rates of $O(^1D)$ by CO_2, N_2, and O_2."

14. W. D. Breshears and P. F. Bird, J. Chem. Phys., 48, 4768 (1968). "Effect of Oxygen Atoms on the Vibrational Relaxation of Nitrogen."

15. G. Herzberg, "Electronic Spectra of Pllyatomic Molecules," D. Van Nostrand Co. (1966).

16. S. D. Peyerimhoff and R. J. Buenker, J. Chem. Phys., 49, 2473 (1968). "Theoretical Study of the Geometry and Spectrum of Nitrous Oxides."

17. G. Herzberg. "Spectra of Diatomic Molecules," second ed., D. Van Nostrand Co. (1950).

18. A. E. Stearn and H. Eyring, J. Chem. Phys., 3, 778 (1935). "Non-adiabatic Reactions. The Decomposition of N_2O."

19. M. Krauss, private communication.

20. N. F. Mott and H. S. W. Massey, "The Theory of Atomic Collisions," third ed., Oxford University Press (1965).

21. T. Yamanouchi and H. Horie, J. Phys. Soc. Japan, 7, 52 (1952). "Intensities of Forbidden Lines of Atoms in p^n-Configurations."

22. E. E. Nikitin, Opt. and Spectr., 9, 8 (1960). "Nonadiabatic Vibrational Excitation of Molecules During Molecular Collisions."

23. E. Bauer, Institute for Defense Analyses, Research Paper P-304, (December 1966). "Quenching of the Resonance Radiation of Sodium by Molecular Nitrogen."
24. J. T. Vanderslice, E. A. Mason and W. G. Maisch, J. Chem. Phys., 31, 738 (1959). "Interactions Between Oxygen and Nitrogen: O-N, O-N_2, O_2-N_2."
25. E. K. Gill and K. J. Laidler, Can. J. Chem., 36, 1570 (1958). "Theoretical Aspects of the Unimolecular Decomposition of Nitrous Oxide."
26. B. G. Reuben and J. W. Linnett, Trans. Farad. Soc. 55, 1543 (1959). "Thermal Decomposition of Nitrous Oxide."
27. H. S. Johnston, J. Chem. Phys., 19, 663 (1951). "Interpretation of the Data on the Thermal Decomposition of Nitrous Oxides."
28. E. Bauer, E. R. Fisher and F. R. Gilmore, Institute for Defense Analyses, Research Paper P-471, (March 1969). "De-Excitation of Electronically Excited Sodium by Nitrogen and Some Other Diatomic Molecules."
29. K. F. Herzfeld and T. A. Litovitz, "Absorption and Dispersion of Ultrasonic Waves," Academic Press (1959).
30. R. C. Millikan and D. R. White, J. Chem. Phys., 39, 3209 (1963), "Systematics of Vibrational Relaxation."
31. K. L. Wray, J. Chem. Phys., 36, 2597 (1962), "Shock Tube Study of the Vibrational Relaxation of Nitric Oxide."

APPENDIX A

PARTIAL QUENCHING CROSS SECTIONS FOR

$$O(^1D) + N_2 \xrightarrow{\sigma(v)} O(^3P) + N_2(v)$$

AS A FUNCTION OF THE COLLISION-MODIFIED FRANCK-CONDON FACTOR*

*All of the cross sections in this Appendix refer to the collision partners $N_2(X\,^1\Sigma_g^+)$ and $O(^1D)$ entering along the lowest possible potential energy curve, i.e., the $^1\Sigma^+$ curve of Fig. 1 or the $^1A'$ curve of Fig. 2. Thus, the total cross sections must be multiplied by the statistical weight factor $g \geq 0.2$--see discussion below Eq. (25).

TABLE A-1. PARTIAL QUENCHING CROSS SECTIONS FOR $O(^1D) + N_2$ REACTION (IN 10^{-16} CM^2)*
BENT (120°) CONFIGURATION

Vibrational Level \ V_{el}**	100 cm^{-1}	300	500
6	0.0	0.0	0.0
5	0.0	0.0	0.0
4	0.0	0.0	0.0
3	0.0	0.0	0.0
2	0.0	0.0	0.0
1	0.0	0.0	0.07
0	1.54	9.50	12.56
Total Quenching Cross Section	1.54	9.50	12.63

* Franck Condon Factor = 0.004 (Corresponds to K = 0.8 in Eq. 23).
Relative kinetic energy = 0.1 ev.

** Assumed spin-orbit interaction.

TABLE A-2. PARTIAL QUENCHING CROSS SECTIONS FOR $O(^1D) + N_2$ REACTION (IN 10^{-16} CM^2)*
BENT (120°) CONFIGURATION**

Vibrational Level \ V_{el}***	100 cm^{-1}	300	500
6	0.0	0.0	0.0
5	0.0	0.0	0.0
4	0.0	0.0	0.0
3	0.0	0.0	0.0
2	0.0	0.0	0.0
1	0.0	0.0	0.20
0	2.16	11.33	11.05
Total Quenching Cross Section	2.16	11.33	11.25

* Franck Condon Factor = 0.004 (Corresponds to K = 0.8 in Eq. 23).
Relative kinetic energy = 0.1 ev.

** 0.7 times effective force terms shown in Table 1. For 120° configuration case.

*** Assumed spin-orbit interaction.

TABLE A-3. PARTIAL QUENCHING CROSS SECTIONS FOR $O(^1D) + N_2$ REACTION (IN 10^{-16} CM^2)*

COLLINEAR CONFIGURATION

Vibrational Level \ V_{el} **	100 cm^{-1}	300	500
6	0.0	0.0	0.0
5	0.0	0.0	0.0
4	0.0	0.0	0.0
3	0.0	0.0	0.0
2	0.0	0.0	0.0
1	0.0	0.0	0.0
0	0.41	3.33	7.60
Total Quenching Cross Section	0.41	3.33	7.60

* Franck Condon Factor = 0.004 (Corresponds to K = 0.8 in Eq. 23). Relative kinetic energy = 0.1 ev.

** Assumed spin-orbit interaction.

TAB.E A-4. PARTIAL QUENCHING CROSS SECTIONS FOR $O(^1D) + N_2$ REACTION (10^{-16} CM^2)*

COLLINEAR CONFIGURATION**

Vibrational Level \ V_{el} ***	100 cm^{-1}	300	500
6	0.0	0.0	0.0
5	0.0	0.0	0.0
4	0.0	0.0	0.0
3	0.0	0.0	0.0
2	0.0	0.0	0.0
1	0.0	0.0	0.0
0	0.58	4.54	9.52
Total Quenching Cross Section	0.58	4.54	9.52

* Franck Condon Factor = 0.004 (Corresponds to K = 0.8 in Eq. 23) Relative kinetic energy - 0.1 ev.

** 0.7 Times effective force terms shown in Table 1 for collinear configuration case.

*** Assumed spin-orbit interaction.

TABLE A-5. PARTIAL QUENCHING CROSS SECTIONS FOR $O(^1D) + N_2$ REACTION (10^{-16} CM^2)*
BENT (120°) CONFIGURATION

Vibrational Level \ V_{el}**	100 cm^{-1}	300	500
6	0.0	0.0	0.0
5	0.0	0.0	0.0
4	0.0	0.0	0.0
3	0.0	0.0	0.0
2	0.0	0.01	0.08
1	0.0	0.33	1.37
0	1.54	9.25	11.76
Total Quenching Cross Section	1.54	9.59	13.21

*Franck Condon Factor = 0.035 (Corresponds to K = 0.4 in Eq. 23). Relative kinetic energy - 0.1 ev.
**Assumed spin-orbit interaction.

TABLE A-6. PARTIAL QUENCHING CROSS SECTIONS FOR $(O(^1D) + N_2$ REACTION (10^{-16} CM^2)*
BENT (120°) CONFIGURATION**

Vibrational Level \ V_{el}***	100 cm^{-1}	300	500
6	0.0	0.0	0.0
5	0.0	0.0	0.0
4	0.0	0.0	0.0
3	0.0	0.0	0.0
2	0.0	0.03	0.12
1	0.0	0.50	2.46
0	2.16	10.91	10.11
Total Quenching Cross Section	2.16	11.44	12.69

*Franck Condon Factor = 0.035 (Corresponds to K = 0.4 in Eq. 23). Relative kinetic energy = 0.1 ev.
**0.7 times effective force terms shown in Table 1 for 120° configuration case.
***Assumed spin-orbit interaction.

TABLE A-7. PARTIAL QUENCHING CROSS SECTIONS FOR $O(^1D) + N_2$ REACTION ($10^{-16} CM^2$)*

COLLINEAR CONFIGURATION

Vibrational Level \ V_{el}**	100 cm^{-1}	300	500
6	0.0	0.0	0.0
5	0.0	0.0	0.0
4	0.0	0.0	0.0
3	0.0	0.0	0.0
2	0.0	0.0	0.01
1	0.0	0.0	0.38
0	0.41	3.33	7.46
Total Quenching Cross Section	0.41	3.33	7.85

* Franck Condon Factor = 0.035 (Corresponds to K = 0.4 in Eq. 23). Relative kinetic energy = 0.1 ev.

** Assumed spin-orbit interaction.

TABLE A-8. PARTIAL QUENCHING CROSS SECTIONS FOR $O(^1D) + N_2$ REACTION (10^{-16} CM^2)* COLLINEAR CONFIGURATION**

Vibrational Level \ V_{el}***	100 cm^{-1}	300	500
6	0.0	0.0	0.0
5	0.0	0.0	0.0
4	0.0	0.0	0.0
3	0.0	0.0	0.0
2	0.0	0.0	0.02
1	0.0	0.22	0.50
0	0.58	4.51	9.26
Total Quenching Cross Section	0.58	4.73	9.78

* Franck Condon Factor = 0.035 (Corresponds to K = 0.4 in Eq. 23). Relative kinetic energy = 0.1 ev.

** 0.7 times effective force terms shown in Table A-1 for collinear configuration case.

*** Assumed spin-orbit interaction.